Journal of the American Heart Association

ORIGINAL RESEARCH

Hypoxia Attenuates Pressure Overload-Induced Heart Failure

Natali Froese, PhD*; Malgorzata Szaroszyk, PhD*; Paolo Galuppo, PhD; Joseph R. Visker, PhD; Christopher Werlein, MD; Mortimer Korf-Klingebiel, PhD; Dominik Berliner, MD; Marc R. Reboll, PhD; Rana Hamouche, MD; Simona Gegel, PhD; Yong Wang, MD; Winfried Hofmann, PhD; Ming Tang, PhD; Robert Geffers, PhD; Adam R. Wende, PhD; Mark P. Kühnel, PhD; Danny D. Jonigk, MD; Georg Hansmann, MD, PhD; Kai C. Wollert, MD; E. Dale Abel, MD, PhD; Stavros G. Drakos, MD, PhD; Johann Bauersachs, MD; Christian Riehle, MD

BACKGROUND: Alveolar hypoxia is protective in the context of cardiovascular and ischemic heart disease; however, the underlying mechanisms are incompletely understood. The present study sought to test the hypothesis that hypoxia is cardioprotective in left ventricular pressure overload (LVPO)–induced heart failure. We furthermore aimed to test that overlapping mechanisms promote cardiac recovery in heart failure patients following left ventricular assist device-mediated mechanical unloading and circulatory support.

METHODS AND RESULTS: We established a novel murine model of combined chronic alveolar hypoxia and LVPO following transverse aortic constriction (HxTAC). The HxTAC model is resistant to cardiac hypertrophy and the development of heart failure. The cardioprotective mechanisms identified in our HxTAC model include increased activation of HIF (hypoxia-inducible factor)-1α–mediated angiogenesis, attenuated induction of genes associated with pathological remodeling, and preserved metabolic gene expression as identified by RNA sequencing. Furthermore, LVPO decreased *Tbx5* and increased *Hsd11b1* mRNA expression under normoxic conditions, which was attenuated under hypoxic conditions and may induce additional hypoxia-mediated cardioprotective effects. Analysis of samples from patients with advanced heart failure that demonstrated left ventricular assist device–mediated myocardial recovery revealed a similar expression pattern for *TBX5* and *HSD11B1* as observed in HxTAC hearts.

CONCLUSIONS: Hypoxia attenuates LVPO-induced heart failure. Cardioprotective pathways identified in the HxTAC model might also contribute to cardiac recovery following left ventricular assist device support. These data highlight the potential of our novel HxTAC model to identify hypoxia-mediated cardioprotective mechanisms and therapeutic targets that attenuate LVPO-induced heart failure and mediate cardiac recovery following mechanical circulatory support.

Key Words: cardiac hypertrophy ■ cardiac remodeling ■ hypoxia ■ left ventricular assist device ■ pressure overload

Heart failure (HF) is the major cause of death in the world with about half of patients dying within 5 years of the initial diagnosis. As such, there is an urgent unmet need to discover new therapies. To identify novel pathways for therapeutic intervention, we focused on intriguing epidemiological studies that reported improved survival for patients with coronary artery disease who live at high altitude being continuously exposed to lower barometric pressure resulting in lower partial pressure of inspired oxygen.[1–3] Furthermore,

Correspondence to: Christian Riehle, MD, Department of Cardiology and Angiology, Hannover Medical School, Carl-Neuberg-Str. 1, 30625 Hannover, Germany. Email: riehle.christian@mh-hannover.de

*N. Froese, M. Szaroszyk, and P. Galuppo contributed equally.

This article was sent to Sakima A. Smith, MD, MPH, Associate Editor, for review by expert referees, editorial decision, and final disposition.

Supplemental Material is available at https://www.ahajournals.org/doi/suppl/10.1161/JAHA.123.033553

For Sources of Funding and Disclosures, see page 15.

JAHA is available at: www.ahajournals.org/journal/jaha

RESEARCH PERSPECTIVE

What Is New?

- We present a novel murine model of combined chronic alveolar hypoxia and left ventricular pressure overload following transverse aortic constriction (HxTAC), which is resistant to the development of heart failure.
- Cardioprotective pathways identified in the HxTAC model might also contribute to cardiac recovery following left ventricular assist device-mediated ventricular mechanical unloading.

What Question Should Be Addressed Next?

- The HxTAC model might serve as a novel tool to identify therapeutic targets that attenuate both left ventricular pressure overload-induced heart failure and mediate cardiac recovery following mechanical circulatory support.

Nonstandard Abbreviations and Acronyms

FAO	fatty acid oxidation
FiO_2	fraction of inspired oxygen
HIF-1α	hypoxia-inducible factor-1α
Hsd11b1	Hydroxysteroid 11-beta dehydrogenase 1
HxSham	hypoxia/sham surgery
HxTAC	Hypoxia/transverse aortic constriction
LVPO	left ventricular pressure overload
NxSham	normoxia/sham surgery
NxTAC	normoxia/transverse aortic constriction
TAC	transverse aortic constriction
Tbx5	T-box transcription factor 5
TCA cycle	tricarboxylic acid cycle

alveolar hypoxia attenuates HF following acute ischemic injury in mice and promotes cardiac recovery in patients following myocardial infarction.[4,5] However, the underlying mechanisms of hypoxia-mediated cardioprotection are incompletely understood.

The HIF (hypoxia-inducible factor)-1 transcription factor complex consists of an oxygen-insensitive β-subunit and an oxygen-sensitive α-subunit, which is hydroxylated under normoxic conditions and targeted for degradation.[6] The HIF-1 complex regulates gene expression of various RNA species, including mRNAs and noncoding RNAs that posttranscriptionally regulate the expression of target transcripts.[7,8] Transgenic overexpression of HIF-1α attenuates HF following myocardial infarction in mice.[9] Furthermore, HIF-1 mediates cardioprotection that is induced by ischemic preconditioning to protect the heart against reperfusion-mediated injury.[10] Transverse aortic constriction (TAC) is a commonly used rodent model to mimic clinical arterial hypertension, aortic valve stenosis, and the evolution of left ventricular (LV) pressure overload (LVPO) and progressive LV hypertrophy toward HF with reduced ejection fraction.[11] Several mouse models with both loss-of-function and gain-of-function HIF-1α gene mutations have been subjected to LVPO; however, the results have not been consistent.[12–15] Importantly, aforementioned animal models do not reflect HIF-1α–independent adaptations at high altitude and alveolar hypoxia. Thus, the effect of alveolar hypoxia in the context of LVPO is not known. We therefore developed a novel murine model of combined chronic alveolar hypoxia by reduced fraction of inspired oxygen (FiO_2) and LVPO induced by TAC (HxTAC).

Similar to alveolar hypoxia, left ventricular assist devices (LVADs) promote cardiac recovery.[5,16–20] LVADs induce ventricular mechanical unloading and circulatory support. LVADs are commonly used as a temporary intervention for patients with advanced HF awaiting heart transplantation (*bridge to transplant*) or as a lifetime therapy when transplant is not an option (destination therapy). Interestingly, a subset of patients with chronic HF will improve cardiac structure and function (LVAD-mediated myocardial recovery) following LVAD support (LVAD responders), ranging from 5% to 60% (average of ≈15%) depending on patient population characteristics, which include HF pathogenesis, duration of disease, age at LVAD implantation, kidney function, and LV dilation.[16–19] The mechanisms contributing to the LVAD-mediated myocardial recovery in these patients are the subject of intensive investigation.[21]

The present study used our novel HxTAC model to test whether alveolar hypoxia is cardioprotective in the context of LVPO and to delineate hypoxia-mediated cardioprotective pathways. Based on cardioprotective mechanisms that are mediated by alveolar hypoxia and LVAD support, we aimed to investigate whether overlapping mechanisms exist that promote cardioprotection in the HxTAC model and contribute to cardiac recovery in patients with HF following LVAD-mediated mechanical unloading and circulatory support.

METHODS

The data that support the findings of this study are available from the corresponding author on reasonable request.

Animal Experiments

Mice were on a pure C57BL/6J genetic background and were randomly assigned to the experimental groups outlined in Figure 1A based on allocation in cages after weaning by animal caretaker staff. Studies were performed in male animals. Mice were housed in cages supplemented with nesting material with a 14-hour light/10-hour dark cycle at 22 °C. Animal well-being was monitored according to score sheets with predefined measures, including breathing, coat, motility, and reaction to stimuli. For tissue harvest, mice were euthanized by cervical dislocation under isoflurane anesthesia. Studies were performed in accordance with protocols approved by local state authorities (Niedersächsisches Landesamt für Verbraucherschutz und Lebensmittelsicherheit, protocol number 18/2999), which conform to the *Guide for the Care and Use of Laboratory Animals* published by the US National Institutes of Health.

Transverse Aortic Constriction

LVPO was induced by TAC in 9-week-old mice.[22] Mice were subcutaneously pretreated with 1 mg/kg buprenorphine (Bayer, Leverkusen, Germany) and 5 mg/kg carprofen (Cp-Pharma, Burgdorf, Germany). Anesthesia was induced with 5% isoflurane, sustained with 2% isoflurane, and monitored by toe pinching. Eye care solution was applied to prevent corneal injury and mice were placed in the supine position on a heating pad (37 °C). Mice were orally intubated and mechanically ventilated using a rodent ventilator (Hugo Sachs Elektronik, March-Hugstetten, Germany). Following horizontal skin incision at the level of the suprasternal notch, the transverse aortic arch was visualized through a median sternotomy. Next, the transverse aortic arch was ligated using a 6–0 silk suture that was tightened around a blunt 25-G needle, which was placed between the innominate artery and the left common carotid artery. The needle was quickly removed, leaving a discrete region of stenosis. The chest and overlying skin were closed. Animals received metamizole (1A Pharma, Holzkirchen, Germany) in the drinking water (200 mg/kg) for 4 days total, starting the day before surgery. The sham procedure was performed identically, except no suture was placed around the aortic arch.

Hypoxia Experiments

Mice were housed under normoxic (21% oxygen in room air) or hypoxic conditions in a hypoxia chamber (BioSpherix, Parish, NY, USA) to mimic lower partial pressure of inspired oxygen present at high altitude. To avoid hypobaropathy, FiO_2 was decreased in the hypoxia chamber by 1%/day from 21% to 12% and was followed by a continuous exposure of 12% oxygen, which mimics an altitude of ≈4200 m above sea level (Figure 1A). Following acclimatization for the duration of 1 week, mice housed under hypoxic conditions were subjected to LVPO by TAC (HxTAC group) or to sham surgery (HxSham group). Mice continuously housed under normoxic conditions post sham surgery (NxSham group) or TAC (NxTAC group) served as controls (Figure 1A). FiO_2 in the hypoxia chamber was automatically adjusted by ventilation and controlled by an OxyCycler controller (BioSpherix). Soda lime (Dräger Medizintechnik, Lübeck, Germany) and activated charcoal (Roth, Karlsruhe, Germany) were used for the removal of CO_2 and ammonia. CO_2 concentration was monitored to not exceed 10 000 ppm (Fuehler Systeme, Nürnberg, Germany).[23] Mice housed under hypoxic conditions received food and water ad libitum. Because hypoxia exposure decreases food intake in mice, mice housed under normoxic conditions were given equivalent amounts of food with unrestricted access to water (*pair-feeding*).[4]

Doppler Velocity Measurements

Peak velocity of the right and left carotid artery was determined to assess TAC-induced pressure gradient. Measurements were performed following anesthesia with isoflurane (1%–2%) and using a 20 MHz Doppler probe coupled to a Vevo 3100 echocardiograph (VisualSonics Inc., Toronto, Ontario, Canada) 2 days post surgery.[24]

Transthoracic Echocardiography

High-resolution 2-dimensional transthoracic echocardiography was performed using an MX 400 transducer coupled to a Vevo 3100 echocardiograph. Two-dimensional B-mode images and endocardial silhouettes were traced manually. Ejection fraction was determined in long-axis projection using the VevoStrain software (VisualSonics Inc., Toronto, Ontario, Canada). LV end-diastolic area and LV end-systolic area were determined in long-axis parasternal projections. Fractional area change was calculated as [(LV end-diastolic area – LV end-systolic area)/LV end-diastolic area]×100. Echocardiographic data and measurements of TAC-induced pressure gradient were obtained from sedated mice for the 2-day time point following anesthesia with isoflurane (1%–2%). Echocardiographic examinations were performed 2 and 4 weeks post surgery in nonsedated mice. The difference in anesthesia protocols emanates from the longer duration for measurements of TAC-induced pressure gradients, which were performed together with echocardiographic exams at the 2-day time point.

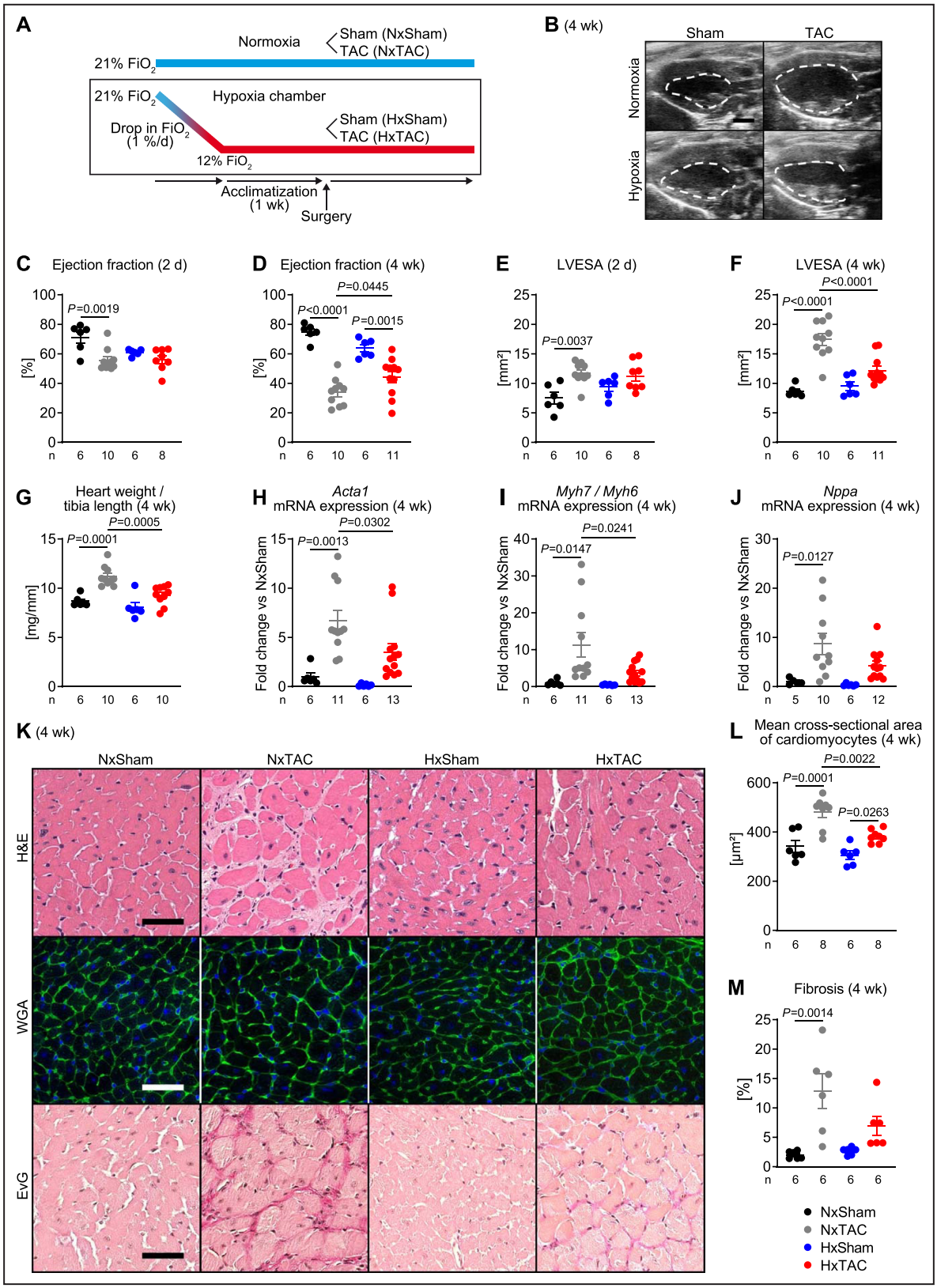

Hemodynamic Studies

Mice were pretreated by intraperitoneal injection of 2 mg/kg butorphanol (Cp-Pharma, Burgdorf, Germany) and subcutaneous injection of 5 mg/kg carprofen. Anesthesia was induced with 3% isoflurane, sustained with 2% to 3% isoflurane, and monitored by toe

Figure 1. Hypoxia attenuates adverse left ventricular remodeling and heart failure following transverse aortic constriction. **A**, Experimental setup with gradual induction of alveolar hypoxia. **B**, Representative B-mode transthoracic echocardiography images at end-systole in long-axis projection 4 weeks post surgery. The dashed line indicates left ventricular end-systolic area (LVESA), scale bars: 2 mm. **C** and **D**, Contractile function determined by ejection fraction 2 days (#) and 4 weeks (#, &) post surgery. **E** and **F**, LVESA 2 days (#) and 4 weeks (#, $, &) post surgery. **G**, Heart weights normalized to tibia length 4 weeks post surgery (#, $). **H** through **J**, mRNA expression of heart failure markers *Acta1*, normalized to *Rps16* (#) *Myh7*/*Myh6* (#), and *Nppa* normalized to *Rps16* (#) 4 weeks post surgery presented as fold change vs NxSham. **K** through **M**, Representative hematoxylin and eosin (H&E), wheat germ agglutinin (WGA), and Elastica van Gieson (EvG) stains (scale bars: 50 μm each) and stereological quantification of mean cross-sectional area of cardiomyocytes (#, $) and fibrotic tissue (#) 4 weeks post surgery. Data are reported as mean±SEM. Two-way ANOVA was performed to analyze differences after TAC by FiO_2, followed by Holm-Šídák post hoc analysis (# $P<0.05$ for TAC, $ $P<0.05$ for FiO_2, and & $P<0.05$ for the interaction between TAC and FiO_2). FiO_2 indicates fraction of inspired oxygen; HxSham, hypoxia/sham surgery; HxTAC, hypoxia/transverse aortic constriction; NxSham, normoxia/sham surgery; NxTAC, normoxia/transverse aortic constriction; and TAC, transverse aortic constriction.

pinching. Mice were placed in the supine position on a heating pad (37 °C), orally intubated, and mechanically ventilated. Following horizontal skin incision at the level of the xyphoid process, the chest was subsequently opened by lateral incisions until the diaphragm was visible from beneath. Next, the diaphragm was opened, the LV apex was punctured using a 25-G needle, and a 1.4 F microtip pressure catheter (Millar Instruments, Houston, TX, USA) was inserted into the LV cardiac apex.[25] LV hemodynamic parameters were recorded using the LabChart software (ADInstrument Ltd. Oxford, UK). LV developed pressure was determined as the difference between LV systolic pressure and LV end-diastolic pressure. Mice were euthanized by cervical dislocation after completion of measurements.

Histological and Immunohistological Analysis

For details see Data S1.

Measurement of Mitochondrial Oxygen Consumption

Mitochondria were isolated from LV tissue and mitochondrial oxygen consumption was determined using a Clark-type oxygen electrode (Strathkelvin, North Lanarkshire, Scotland) as previously described.[26,27]

Mitochondrial Enzyme Activity Assays

Citrate synthase and hydroxyacyl-coenzyme A dehydrogenase enzyme activities were measured as previously described using a Synergy HT multidetection microplate reader (BioTek Instruments, Winooski, VT, USA) with a total reaction volume of 200 μL.[28]

Measurement of Mitochondrial DNA Content

DNA was extracted from LV tissue using DirectPCR Lysis Reagent (Viagen Biotech, Inc., Los Angeles, CA, USA) containing 0.8 μg/μL Proteinase K (Merck, Darmstadt, Germany) according to the manufacturers' instructions, which was followed by ethanol precipitation. DNA was dissolved in 50 μL of 10 mmol/L Tris–HCl (pH 8.0). Next, 10 ng of total DNA was subjected to quantitative polymerase chain reaction analysis. The mitochondrial DNA content relative to nuclear DNA content was determined using the following primers: mitochondrial DNA-encoded *cytochrome c oxidase 1*: forward 5′-ACTATACTACTAACAGACCG-3′, reverse 5′-GGTTCTTTTTTTCCGGAGTA-3′; and nuclear DNA-encoded *cyclophilin A*: forward 5′-ACACGCCATAA TGGCACTGG-3′, reverse 5′-CAGTCTTGGCAGTG CAGAT-3′.

Hemoglobin Analysis

Blood samples were collected by submandibular bleed and hemoglobin analysis was performed using an ABL800 FLEX blood gas analyzer (Radiometer Medical ApS, Brønshøj, Denmark).

Immunoblotting Analysis

For details see Data S1.

RNA Sequencing and Quantitative Reverse Transcription-Polymerase Chain Reaction/HxTAC Model

For details see Data S1.

Human Subjects

For details see Data S1. Studies were approved by the institutional review board (protocol number #30622) of the Utah Cardiac Recovery Program (UCAR; University of Utah Health & School of Medicine, Intermountain Medical Center, and Salt Lake City VA Medical Center, Salt Lake City, UT). All patients provided informed consent before participation.

Statistical Analysis

Data are expressed as mean±SEM. For murine studies, data sets were analyzed by 2-way ANOVA for multigroup comparisons with Holm-Šídák post hoc

analysis to determine significance levels between surgery and FiO_2. Whenever possible, investigators were blinded to group allocation during experiments performed and further analyses. Only mice that survived until the predefined time point of tissue harvest were included in molecular analyses. Sample size for murine studies was determined based on our previous experience with murine LVPO models following TAC surgery and gene profiling by RNA sequencing.[27,29,30] Analysis of RNA sequencing data from patients with advanced HF was performed based on data availability using a previously published data set.[20] Statistical analyses were performed using GraphPad Prism software version 8.0 (GraphPad Software, San Diego, CA) and for RNA sequencing data as described in detail in Data S1. Grubbs' test was used to identify outliers in data sets. For all analyses, a P value of <0.05 was considered significantly different. P values for significant differences are indicated (cutoff: P<0.05).

RESULTS

Hypoxia Attenuates TAC-Induced Adverse LV Remodeling and HF

TAC increased hemodynamic stress independent of FiO_2 as determined by peak velocity measured from the right and left carotid arteries (Figure S1) and LV developed pressure 3 days post surgery (Table S1). Hypoxia increased serum hemoglobin independent of the surgery performed (Table S2). Two days post TAC, NxTAC exhibited contractile dysfunction as evidenced by impaired ejection fraction relative to NxSham. NxTAC developed overt HF 4 weeks post-surgery as indicated by decreased ejection fraction, increased LV end-systolic area (Figure 1B through 1F, Table S3), cardiac hypertrophy as indicated by an increase in heart weight/tibia length ratio (Figure 1G and Table S4), increased mRNA expression of HF markers (Figure 1H through 1J), and evidence of adverse remodeling including cellular hypertrophy and fibrosis (Figure 1K through 1M). Importantly, these effects were attenuated in HxTAC. HxSham exhibited no overt cardiac phenotype compared with NxSham controls (Figure 1B through 1M and Tables S1, S3, S4). Stereological analysis showed no increase in cardiomyocyte count in HxSham relative to NxSham hearts (data not presented), thus indicating no cardiomyocyte proliferation in mice housed under hypoxic conditions under basal conditions. Interestingly, proapoptotic, autophagic, and mitophagic signaling was not different between groups (Figure S2). Together, these data demonstrate that hypoxia exposure attenuates TAC-induced adverse LV remodeling and HF.

Hypoxia Promotes HIF-1α Expression and Angiogenesis

Both LVPO and HIF-1 induce angiogenesis, which preserves contractile function post TAC.[12,31] To test whether the beneficial effects of hypoxia under LVPO conditions are transduced by increased HIF-1 transcriptional activity and angiogenesis, we measured HIF-1α protein abundance and mRNA expression of its transcriptional target *Vegfa*, a master regulator of angiogenesis. At the 2-week time point, HIF-1α protein expression was increased in the NxTAC and the HxSham groups relative to NxSham with a further increase in the HxTAC group compared with NxTAC. No difference in HIF-1α expression between groups was observed for the 3-day and 4-week time points (Figure 2A and 2B). *Vegfa* mRNA expression was increased in HxSham hearts at the 4-week time point and trended to further increase in HxTAC relative to NxTAC (+40.3%, P=0.077). No difference in *Vegfa* mRNA expression between groups was detected 3 days and 2 weeks post surgery (Figure 2C). Hypoxia increased the number of capillaries per area under Sham conditions (HxSham versus NxSham: +22.8%) with a further increase post TAC (HxTAC versus HxSham: +24.2%, Figure 2D and 2E). These data suggest that hypoxia promotes cardioprotective effects under hypoxic conditions, at least in part, by increasing angiogenesis.

Hypoxia Attenuates the Transcriptional Response of Pathological Remodeling and Preserves Post-TAC Metabolic Gene Expression

To comprehensively assess the cardioprotective mechanisms in the HxTAC model, we performed differential gene expression analysis by bulk RNA sequencing using LV tissue. The experiment was performed at the 3-day time point representing an early phase in ventricular remodeling when contractile function was similar following TAC in normoxic and hypoxic groups (Figure 1C and Tables S1 and S3). Principal component analysis and differential gene expression analysis revealed that gene expression patterns for NxSham and HxSham hearts were relatively similar, whereas samples for NxTAC and HxTAC exhibited distinct clusters (Figure 3A and Data S2). We detected a total of 2378 genes that were induced and 1267 that were repressed in the NxTAC compared with the NxSham group (cutoff: $|\log_2$ fold change$|$ >0.6 and P<0.05). Similarly, 1577 genes were induced and 1078 were repressed in the HxTAC relative to HxSham group (cutoff: $|\log_2$ fold change$|$ >0.6 and P<0.05; Figure 3B). Gene expression was robustly different between groups, as shown by heatmap (Figure 3C). To identify hypoxia-regulated cardioprotective transcripts, we next focused

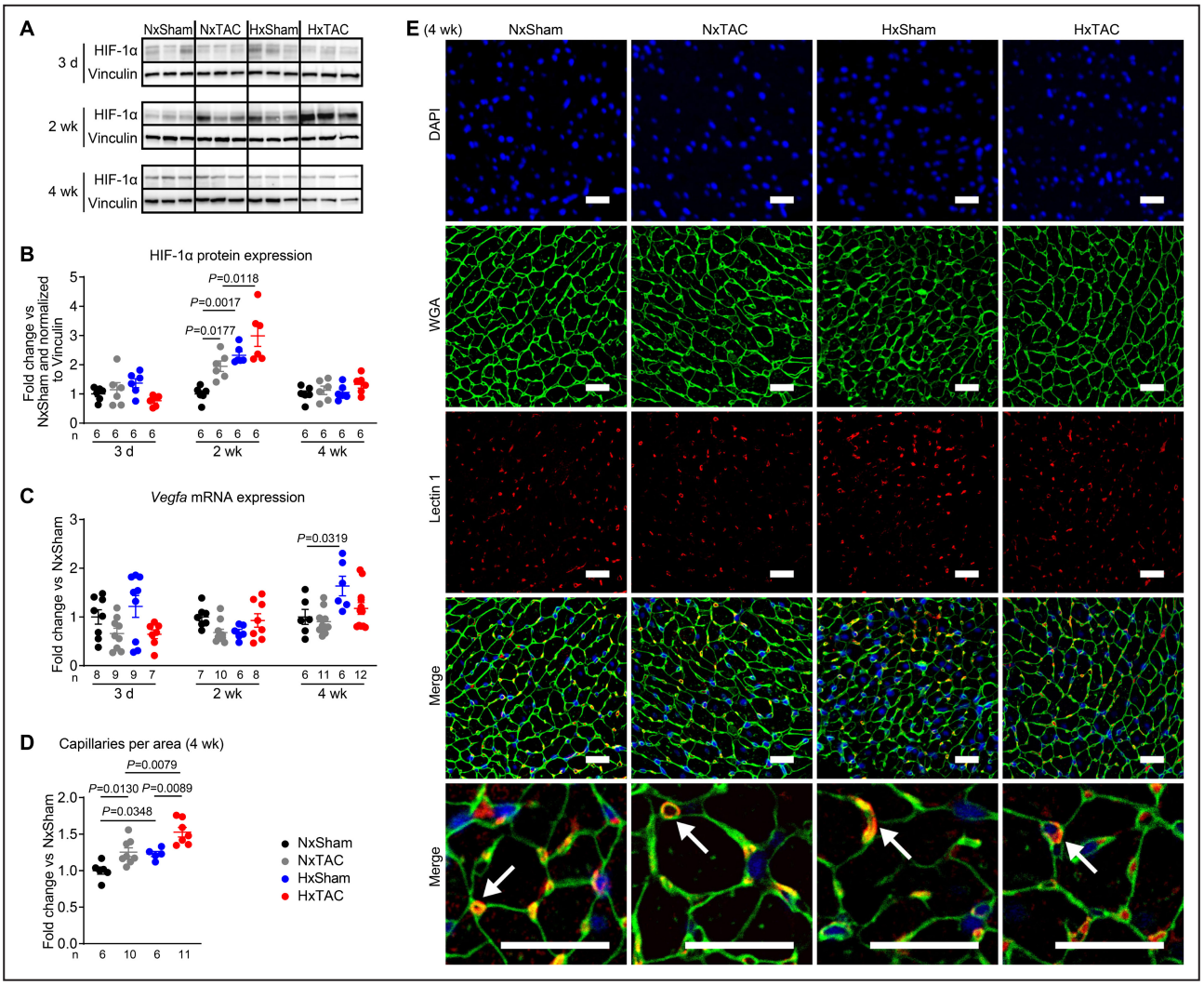

Figure 2. Hypoxia induces HIF-1α expression and angiogenesis.
A and **B**, Representative immunoblots in left ventricular homogenates and densitometric quantification of HIF-1α protein expression normalized to vinculin 3 days (&), 2 weeks (#, $), and 4 weeks post surgery. **C**, *Vegfa* mRNA expression normalized to *Rps16* 3 days (#), 2 weeks (&), and 4 weeks (#, $) post surgery. **D** and **E**, Quantification of capillary density per area and representative images 4 weeks post surgery (#, $; scale bars: 30 μm). Arrows indicate organized capillaries. Data are reported as mean±SEM and as fold change relative to NxSham at the same time point post surgery. Two-way ANOVA was performed to analyze differences after transverse aortic constriction (TAC) by fraction of inspired oxygen (FiO_2), followed by Holm-Šídák post hoc analysis (# $P<0.05$ for TAC, $ $P<0.05$ for FiO_2, and & $P<0.05$ for the interaction between TAC and FiO_2). HIF-1α indicates hypoxia-inducible factor-1α; HxSham, hypoxia/sham surgery; HxTAC, hypoxia/transverse aortic constriction; NxSham, normoxia/sham surgery; NxTAC, normoxia/transverse aortic constriction; and WGA, wheat germ agglutinin.

on genes that have been associated with adverse remodeling and myocardial energetics.[32]

Hypoxia attenuated the transcriptional response that characterizes adverse LV remodeling post TAC (Figure 4), including the myosin isoform switch from α myosin heavy chain (*Myh6*) to β myosin heavy chain (*Myh7*), which is a hallmark of TAC-induced HF.[33] We identified 11 genes associated with pathological remodeling that were induced and 9 that were repressed in the NxTAC relative to the NxSham group. Interestingly, 9 transcripts were repressed (4 induced) in the HxTAC relative to the NxTAC group (cutoff: false discovery rate <0.1 each; Figure 4). LVPO is characterized by decreased fatty acid oxidation (FAO) and increased glycolytic flux.[34,35] We identified 16 FAO genes that were repressed in the NxTAC relative to NxSham group. *Acsl5* and *Acsl4* were the only significantly induced FAO genes in the same comparison. Importantly, FAO gene expression was relatively preserved in HxTAC relative to HxSham hearts with 2 genes significantly induced and 4 genes significantly repressed. Interestingly, expression of *Hadh*, *Acadm*, and *Cpt1b*, which are critical for myocardial FAO, was decreased in NxTAC relative to NxSham hearts, and

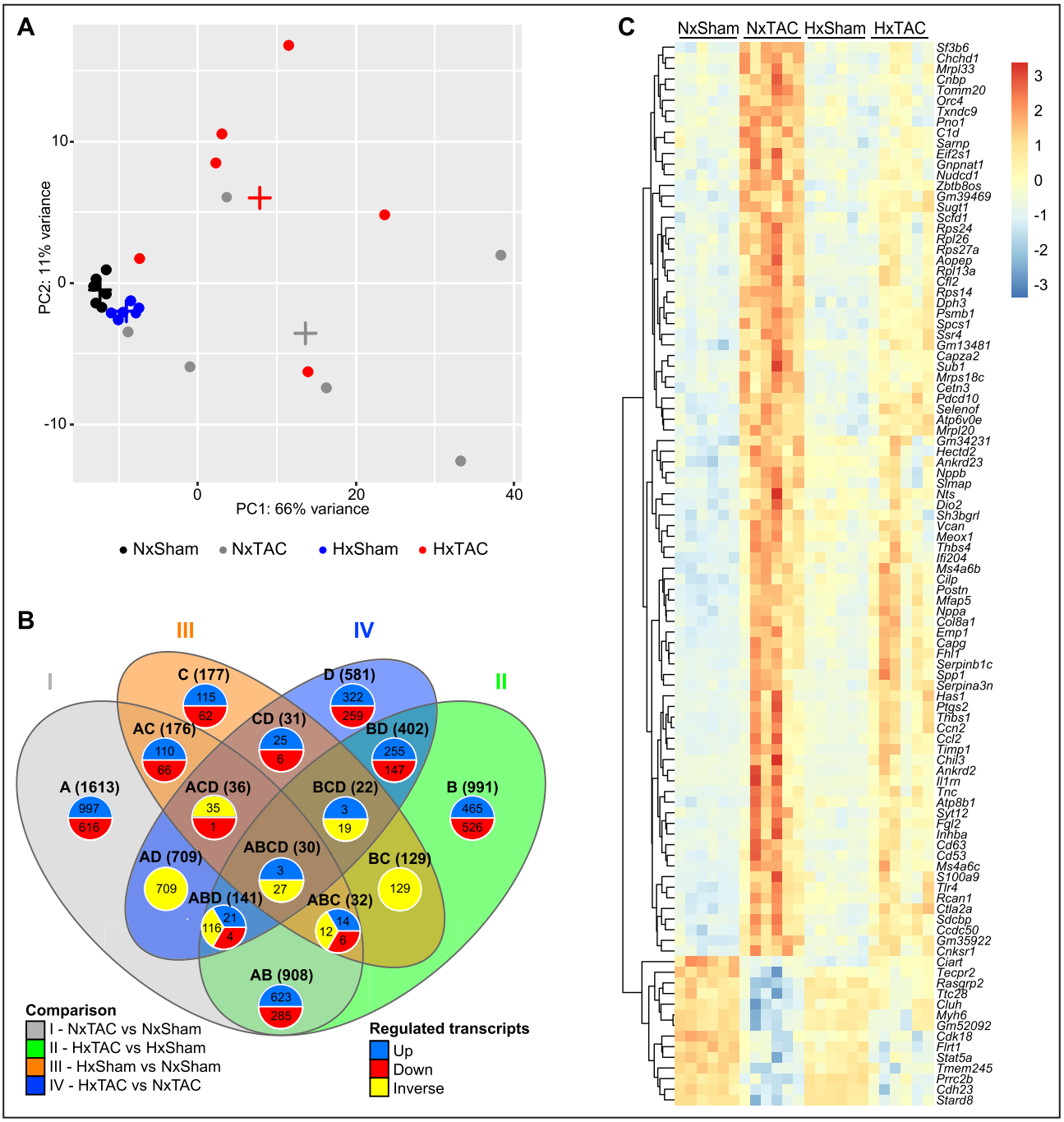

Figure 3. Gene expression 3 days post surgery as determined by RNA sequencing.
A, Principal component analysis to visualize global gene expression clusters by surgery and fraction of inspired oxygen (FiO_2; n=6). Crosses indicate the center of the corresponding clusters. **B**, Venn diagram illustrating the number of altered transcripts (cutoff: $|\log_2$ fold change$|$ >0.6 and P<0.05). **C**, Heatmap of RNA sequencing count data corresponding to the 100 genes with the greatest variance across samples. Data are clustered by row after applying the regularized log transformation function in DESeq2. HxSham indicates hypoxia/sham surgery; HxTAC, hypoxia/transverse aortic constriction; NxSham, normoxia/sham surgery; and NxTAC, normoxia/transverse aortic constriction.

this effect was not observed in LVPO under hypoxic conditions. Under normoxic conditions, 6 tricarboxylic acid (TCA) cycle genes (ie, *Cs*, *Dlst*, *Ogdh*, *Sdha*, *Aco1*, and *Idh3a*) were decreased post TAC, whereas no TCA cycle transcript was increased. Similar to the expression pattern observed for FAO genes, TCA genes were relatively preserved for the comparison HxTAC versus HxSham (1 increased/1 decreased, cutoff: false discovery rate <0.1 each; Figure 5A). Interestingly, *Cs*, *Dlst*, *Sdha*, *Aco1*, and

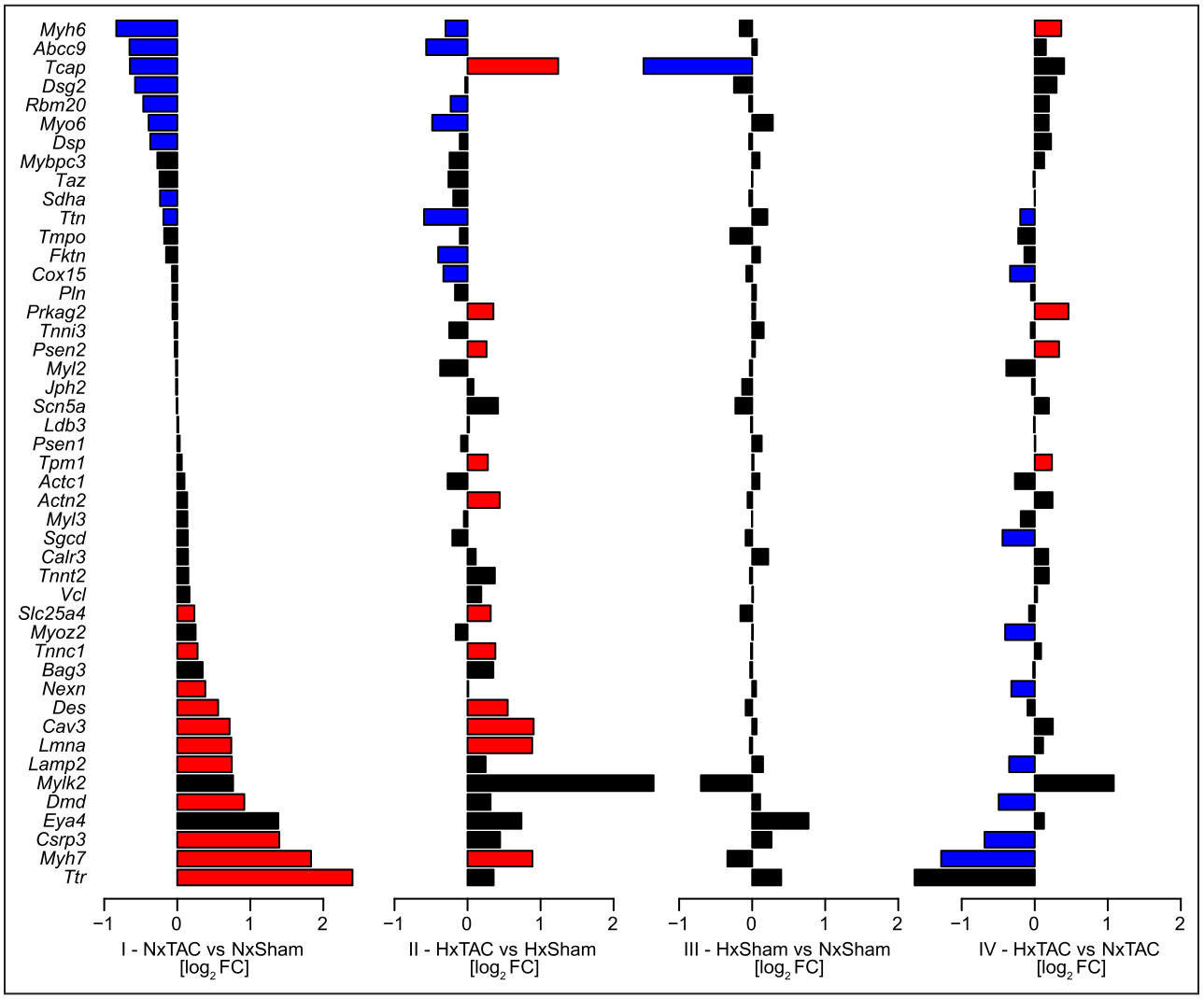

Figure 4. Hypoxia attenuates the transverse aortic constriction-induced transcriptional response of pathological remodeling 3 days post surgery.

Data are presented as mean values for the comparisons as indicated (n=6). Blue and red bars indicate down- and upregulated, respectively. Black bars are not regulated (cutoff: false discovery rate <0.1). FC indicates fold change; HxSham, hypoxia/sham surgery; HxTAC, hypoxia/transverse aortic constriction; NxSham, normoxia/sham surgery; and NxTAC, normoxia/transverse aortic constriction.

Idh3a expression was not decreased post TAC under hypoxic conditions. A total of 9 glycolytic genes were increased and 8 were decreased for the comparison NxTAC versus NxSham. Our analysis identified 8 glycolytic transcripts that were increased for the comparison HxTAC versus HxSham (2 decreased) and 7 glycolytic transcripts that were increased (2 decreased) in HxTAC relative to NxTAC hearts (Figure 5A). In the absence of the superimposed stressor of TAC and as indicated by the comparison HxSham versus NxSham, alveolar hypoxia had no impact on HIF-1α target gene expression involved in glucose oxidation, including GLUT1 (glucose transporter 1, *Slc2a1*), hexokinase 2 (*Hk2*), and *Gapdh*, which is supported by our cumulative distribution analysis (Figure S3). Expression of PGC (peroxisome proliferator-activated receptor-γ coactivator)-1α (*Ppargc1a*), a master regulator of mitochondrial biogenesis and gene expression, was not different between groups (Figure 5B). mRNA expression of pyruvate dehydrogenase kinase 4 (*Pdk4*), which phosphorylates pyruvate dehydrogenase and inhibits glucose oxidation, was decreased in the NxTAC and HxSham groups relative to NxSham. No statistical significant difference was detected in the HxTAC relative to the NxTAC and HxSham groups (Figure 5C).

Based on our results from the RNA sequencing experiment, we next assessed the impact of alveolar hypoxia and LVPO on mitochondrial energetics. Mitochondrial state III oxygen consumption

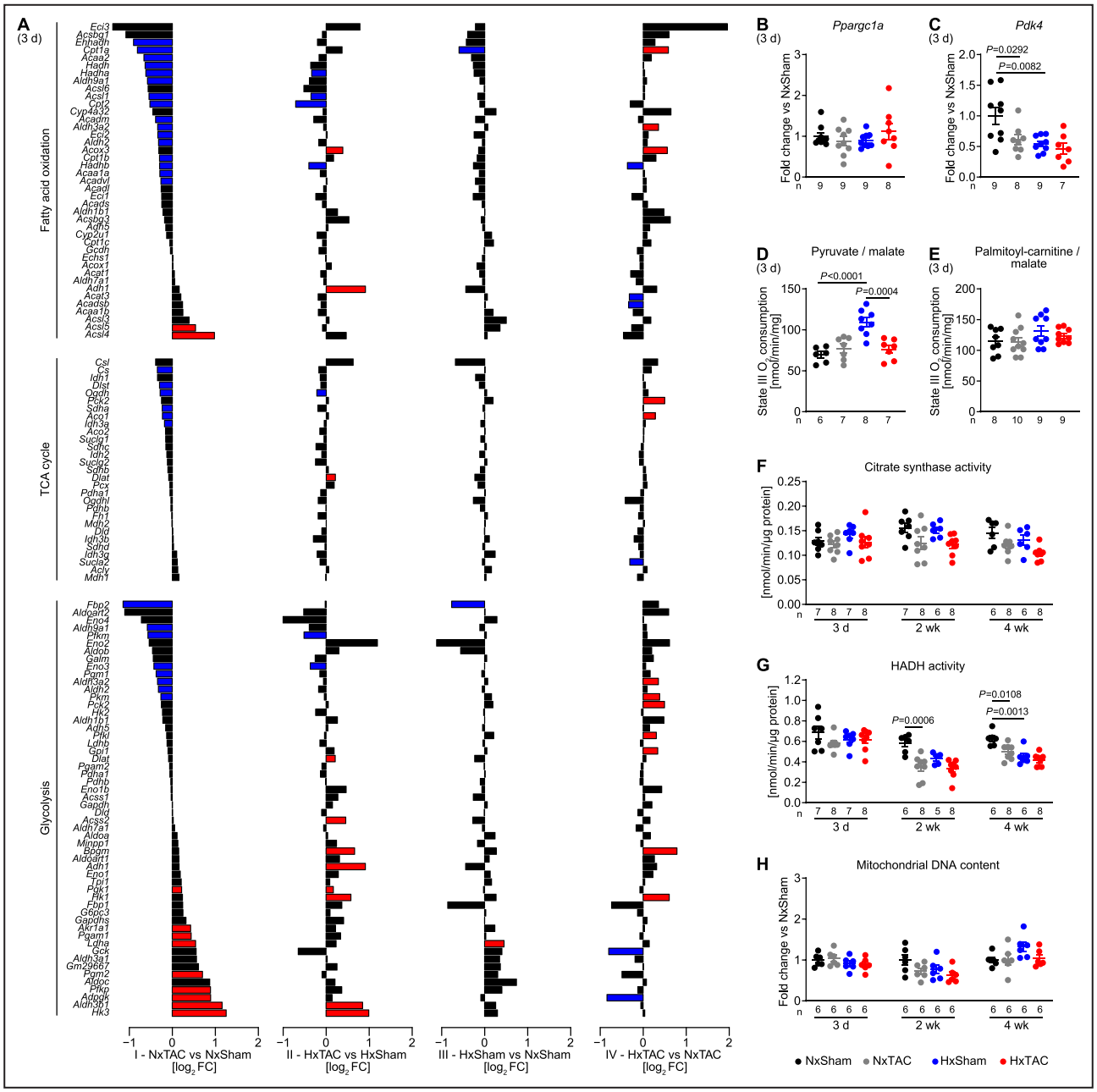

Figure 5. Hypoxia attenuates the transcriptional response of metabolic genes 3 days post transverse aortic constriction. **A**, Expression of transcripts involved in fatty acid oxidation, tricarboxylic acid (TCA) cycle, and glycolysis 3 days post surgery presented as mean values for the comparisons as indicated (n=6). Blue and red bars indicate down- and upregulated, respectively. Black bars indicate not regulated (cutoff: false discovery rate <0.1). **B** and **C**, mRNA expression of *Ppargc1a* and *Pdk4* (#, $) normalized to *Gapdh* ($) 3 days post surgery as determined by quantitative reverse transcription-polymerase chain reaction (qPCR) analysis. **D** and **E,** Mitochondrial state III oxygen consumption with pyruvate (#, $, &) and palmitoyl-carnitine each combined with malate as substrates 3 days post -surgery. **F**, Citrate synthase enzyme activity in left ventricular (LV) tissue 3 days, 2 weeks (#), and 4 weeks (#) post surgery. **G**, Hydroxyacyl-coenzyme A dehydrogenase (HADH) enzyme activity in LV tissue 3 days, 2 weeks (#, $) and 4 weeks (#, $) post surgery. **H**, Mitochondrial DNA content in LV tissue 3 days, 2 weeks (#) and 4 weeks post surgery. Data are presented as mean values ± SEM. Two-way ANOVA was performed to analyze differences after TAC by fraction of inspired oxygen (FiO_2), followed by Holm-Šídák post hoc analysis (# $P<0.05$ for TAC, $ $P<0.05$ for FiO_2, and & $P<0.05$ for the interaction between TAC and FiO_2). HxSham indicates hypoxia/sham surgery; HxTAC, hypoxia/transverse aortic constriction; NxSham, normoxia/sham surgery; and NxTAC, normoxia/transverse aortic constriction.

with pyruvate/malate as substrates was increased in the HxSham compared with the NxSham group. Interestingly, no difference between the HxTAC and the NxTAC group was detected using the same substrate combination (Figure 5D). Mitochondrial oxygen consumption with palmitoyl-carnitine/malate as substrates, activity of the mitochondrial enzymes citrate synthase, mitochondrial DNA content, and abundance

of proteins involved in mitochondrial dynamics were not different between groups. Hydroxyacyl-coenzyme A dehydrogenase enzymatic activity was not different between groups at the 3-day time point; however, it was decreased in the NxTAC compared with the NxSham group at the 2-week and 4-week time points. Furthermore, we detected a statistically significant decrease in the HxSham compared with the NxSham group with no further decrease for the comparison HxTAC versus HxSham at the 4-week time point (Figure 5E through 5H and Figure S4). Oxidative stress was assessed by 4-HNE (4-hydroxynonenal) and MnSOD (mitochondrial superoxide dismutase) protein expression. No statistically significant difference between groups was detected at the time points investigated (Figure S5). Together, these data identify a transcriptional program by which hypoxia attenuates pathological remodeling and preserves metabolic gene expression in LVPO that is independent of mitochondrial energetics and oxidative stress, which might attenuate the onset of HF in HxTAC hearts.

Identification of Potential Mechanisms that Attenuate HF in the HxTAC Model and May Mediate Myocardial Recovery Following LVAD Support

Our data raise the intriguing question of whether the mechanisms by which alveolar hypoxia attenuates LVPO-induced HF in mice also mediate cardiac recovery of a subset of patients following LVAD support. To identify genes that are either protective or adverse in both the HxTAC model and following LVAD-mediated myocardial recovery, we compared the RNA sequencing data set from the HxTAC model with transcriptomics from patient samples that were obtained from the LV apical core at the time of LVAD implantation.[20] To identify potential protective transcripts, we focused our analysis on genes that were *decreased* in LVAD non-responders compared with LVAD responders, *decreased* under normoxic conditions post TAC, and *increased* in HxTAC relative to NxTAC. To identify potential adverse transcripts, we focused on genes that were *increased* in LVAD non-responders relative to LVAD responders, *increased* post TAC under normoxic conditions, and *decreased* in HxTAC relative to NxTAC (Figure 6A). After applying these selection criteria and following quantitative polymerase chain reaction verification of murine HxTAC model samples, we identified T-box transcription factor 5 (*TBX5*, *Tbx5*) as a potential protective and Hydroxysteroid 11-beta dehydrogenase 1 (*HSD11B1*, *Hsd11b1*) as a potential adverse transcript (Figure 6B through 6E). Both transcripts have been associated with the pathogenesis of HF.[36–40] Together, these data suggest that transcripts that correlate with attenuation of HF in the HxTAC model might also regulate pathways that contribute to recovery in a subset of patients following LVAD-mediated circulatory support (Figure 6B through 6E).

DISCUSSION

Hypoxia-mediated cardioprotective mechanisms in the context of cardiovascular and ischemic heart disease are incompletely understood. The present study describes the novel HxTAC model to identify alveolar hypoxia-mediated cardioprotective mechanisms in the context of LVPO. Interestingly, hypoxia-mediated cardioprotective pathways identified in the HxTAC model might also contribute to cardiac recovery following LVAD-mediated mechanical circulatory support in patients with advanced HF.

The impact of high altitude and atmospheric hypoxia on the development of cardiovascular disease has been investigated in epidemiological studies with some reporting protective effects for alveolar hypoxia and others opposing this.[41,42] Parameters that contribute to the outcome of these studies include environmental and genetic factors, access to health care, the duration of high altitude exposure, and ethnicity. These factors, which are very difficult to distinguish from those that are attributable exclusively to high altitude, have not been adequately addressed in the design and analysis of some of the previous studies and thus might have confounded the results.[42] A study investigating the Swiss National Cohort Study Group, which comprises a relatively homogeneous population with access to universal health care, reported a reduced risk for high altitude exposure on coronary heart disease and stroke mortality.[1] A follow-up study using the same cohort showed that the beneficial effect of high altitude on ischemic heart disease persisted after adjusting for environmental factors.[3] Similarly, high altitude is beneficially associated with ischemic heart disease mortality in a US study population after adjusting for sociodemographic factors, exposure to solar radiation, migration, and smoking.[43] In the present study, mice exposed to hypoxia were subjected to TAC, which mimics hypertension and aortic valve stenosis in humans. One potential caveat to be acknowledged is the immediate onset of LVPO post-TAC that is in contrast to the slow disease progression in humans.[11] The identified hypoxia-mediated cardioprotective mechanisms in the HxTAC model include increased angiogenesis, attenuated pathological remodeling, and preserved metabolic gene expression as identified by gene profiling.

A previous study reported increased cardiac regeneration in adult mice following myocardial infarction that were subjected to severe hypoxia with 7% FiO_2. The identified mechanisms include impaired mitochondrial oxidative metabolism, which decreases cardiomyocyte

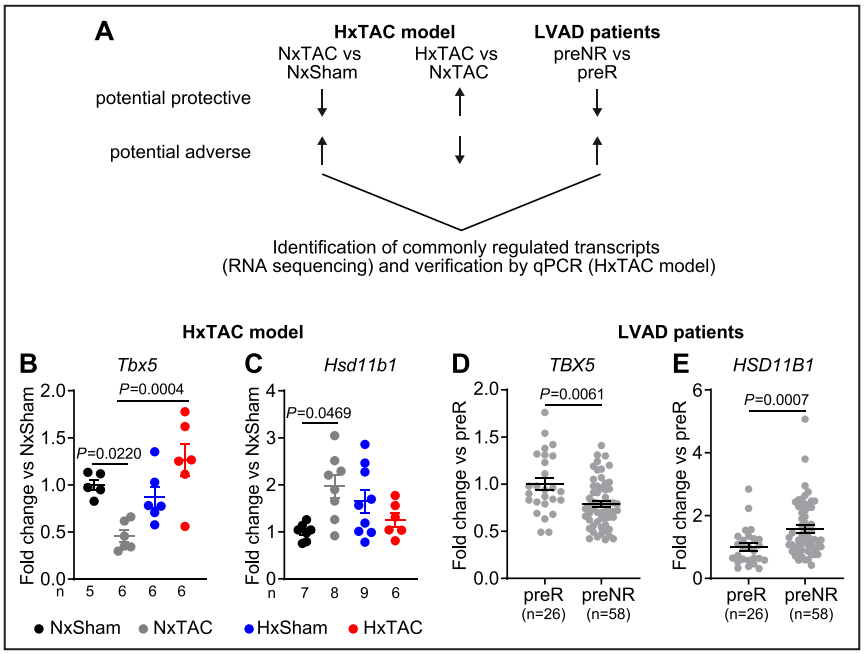

Figure 6. Commonly regulated transcripts in the HxTAC model and patients with cardiac recovery following left ventricular assist device-mediated circulatory support.

A, Methodological approach for the identification of transcripts that are either protective or adverse in both LVAD-mediated mechanical circulatory support and the HxTAC model. **B** and **C**, mRNA expression of *Tbx5* ($, &) and *Hsd11b1* (&) normalized to *Gapdh* 3 days post surgery as determined by quantitative reverse transcription-polymerase chain reaction (qPCR) analysis. Data are reported as mean±SEM and as fold change relative to NxSham at the same time point post surgery. Two-way ANOVA was performed to analyze differences after transverse aortic constriction (TAC) by fraction of inspired oxygen (FiO_2), followed by Holm-Šídák post hoc analysis ($ $P<0.05$ for FiO_2 and & $P<0.05$ for the interaction between TAC and FiO_2). **D** and **E**, mRNA expression of *TBX5* and *HSD11B1* in preNR relative to preR as determined by RNA sequencing. Data are reported as mean±SEM. HxSham indicates hypoxia/sham surgery; HxTAC, hypoxia/transverse aortic constriction; LVAD, left ventricular assist device; NxSham, normoxia/sham surgery; NxTAC, normoxia/transverse aortic constriction; preR, LVAD responders (ie, recovery); and preNR, LVAD non-responders (ie, no recovery post LVAD implantation).

reactive oxygen species production and promotes cardiomyocyte proliferation.[4] Furthermore, alveolar hypoxia promotes cardiac regeneration in patients following myocardial infarction.[5] The present study uses a relatively mild hypoxia protocol with 12% FiO_2. Our stereological analysis revealed no increase in cardiomyocyte count in HxSham relative to NxSham hearts, which indicates that mild hypoxia attenuates LVPO-induced HF by mechanisms that are independent of cardiomyocyte proliferation. Similarly, mild hypoxia with 10% FiO_2 had only modest effects on cardiomyocyte proliferation and did not improve contractile function following myocardial infarction.[4] Our study suggests that mild hypoxia exposure (12% FiO_2) has no impact on oxidative stress (Figure S5). Of note, mild hypoxia as used in the present study better reflects the adaptations of individuals living at high altitude. Severe hypoxia (7% FiO_2), which is equivalent to chronic hypoxia at the summit of Mount Everest, is poorly tolerated by mice over longer time periods and increases mortality after 3 weeks of exposure.[4] Together, these data indicate that different mechanisms mediate the protective effects of mild and severe hypoxia.

HIF-1 transcriptional activity is increased under hypoxic conditions and mediates energetic gene expression.[6] HIF-1α mediates the expression of *Slc2a1* and glycolytic enzymes, including *Hk2*, which shift carbon substrate flux from the TCA cycle to the lactate dehydrogenase A reaction to preserve energy supply at low oxygen concentrations. The subsequent reduction in flux through the mitochondrial electron transport chain and oxidative phosphorylation decreases mitochondrial reactive oxygen species production.[44] Importantly, these mechanisms have mainly been described in vitro.[45–47] Gene expression analysis revealed no impact of hypoxia on HIF-1α target gene expression under nonstressed conditions; however, increased HIF-1α–mediated transcription post TAC independent

of FiO_2. One potential mechanism for this observation are the immediate adaptations post TAC that might increase HIF-1α transcriptional activity independent of HIF-1α protein expression (Figure 2A and 2B).

The temporary increase in HIF-1α protein expression 2 weeks post TAC (Figure 2A and 2B) is similar to a previous study reporting increased HIF-1 activity between 3 days and 14 days post TAC that might be critical for the adaptive mechanism to LVPO.[12] The difference in the time course of HIF-1 activity and expression between this earlier study and our study might result from the variable responses of mice subjected to LVPO that are secondary to differences in genetic background or differences in surgical protocols.[11,12] In the present study, the increase in *Vegfa* mRNA expression and increased capillary density 4 weeks post surgery suggests cardioprotective HIF-1α–mediated angiogenesis in HxTAC hearts (Figure 2). LVPO decreases mitochondrial substrate oxidation and increases glycolytic flux, which is in concert with the present study reporting a repression of mitochondrial FAO and TCA cycle genes post-TAC under normoxic conditions.[34,35] We identified a PGC-1α–independent transcriptional program by which hypoxia preserves metabolic gene expression post-TAC, which might attenuate HF in HxTAC hearts (Figure 5A and 5B). Interestingly, mitochondrial energetics was not different in the HxTAC compared with the NxTAC group (Figure 5D through 5H). The early induction of glycolytic genes together with preserved TCA and FAO gene expression provides a potential mechanism for attenuated future onset of HF in HxTAC hearts. It is of great interest to assess cardiac substrate use in the HxTAC model, which is the subject of future studies.

The present study uses a protocol of mild hypoxia exposure, in which mice were acclimatized to hypoxia before TAC. Our experimental setting is comparable to a scenario, in which individuals living at high altitude exhibit a decreased risk of cardiovascular disease.[1,3,43] The beneficial effect of mild alveolar hypoxia exposure in patients with HF is supported by a pilot study reporting improved exercise time, skeletal muscle strength, and a trend toward improved LV contractile function, which were sustained after 1 month after completion of altitude exposure. The protocol comprised 10 sessions over a period of 22 days starting with a FiO_2 that is comparable to an altitude of 1500 m and increased by 300 m with each subsequent session until a FiO_2, which mimics a maximum altitude of 2700 m, was reached.[48] Despite potential chronic altitude-associated cardioprotective effects, the *acute* reduction in exercise performance under hypoxic conditions is important to consider for future clinical studies with patients with HF and impaired exercise capacity.[49,50] The present study excluded patients with hypertrophic cardiomyopathy. Based on different mechanisms of pathogenesis that result in HF, that is, genetic disorders that result in cardiac hypertrophy in patients with hypertrophic cardiomyopathy and TAC-induced LVPO in mice, patients with hypertrophic cardiomyopathy were excluded from the analysis.[11,51]

We identified *Tbx5* as a potential protective transcript in both HxTAC hearts and LVAD responders (Figure 6). *Tbx5* is a member of the T-box transcription factor family with an essential role for physiological cardiac and forelimb development.[52] *Tbx5* expression is critical for cardiac conduction system development and function.[36,37] *Tbx5* interacts with GATA4 to mediate *Myh6* expression, and perturbed interaction between these 2 transcription factors causes congenital heart defects.[38,53,54] Similarly, we observed reduced *Myh6* expression post-TAC under normoxic conditions, which was attenuated by hypoxia (Figure 4). *Hsd11b1* was identified as a potential adverse transcript in the present study (Figure 6). *Hsd11b1* catalyzes the generation of glucocorticoids from their intrinsically inert metabolites, which increases intracellular and tissue glucocorticoid levels.[55] Genetic deletion of *Hsd11b1* improves outcome following ischemic injury in mice.[39,40] Importantly, the relationship between *Tbx5* and *Hsd11b1* in the context of LVPO and mechanical unloading remains to be determined. Modulation of the expression and activity of *Tbx5* and *Hsd11b1* might be a promising approach to improve cardiac function in LVPO, mechanical unloading, and circulatory support. Together, our data highlight the potential of the HxTAC model as a discovery tool to identify cardioprotective mechanisms also in the context of different stressors. This intriguing possibility is of great interest for the design of future studies.

Study Limitations

One limitation of the present study is that only male mice have been studied. Male rodents are more susceptible to the onset of LVPO-induced heart failure compared with female rodents, which has been associated with sex-specific differences in gene expression.[56] Another limitation is that gene profiling was performed in LV tissue. Thus, we cannot discern the impact of LVPO and alveolar hypoxia on gene expression in the different cellular populations of the heart. Based on technical limitations, transthoracic echocardiographs, Doppler velocity measurements, and surgical procedures in the HxSham and HxTAC groups were not performed in the hypoxia chamber, which might have confounded the results reported in the present study. Even though not directly proven, it is unlikely that short-term removal of mice from the hypoxic environment has a significant impact on the results reported. This assumption is based on the duration of chronic hypoxia exposure of up to several weeks reported in the present study compared

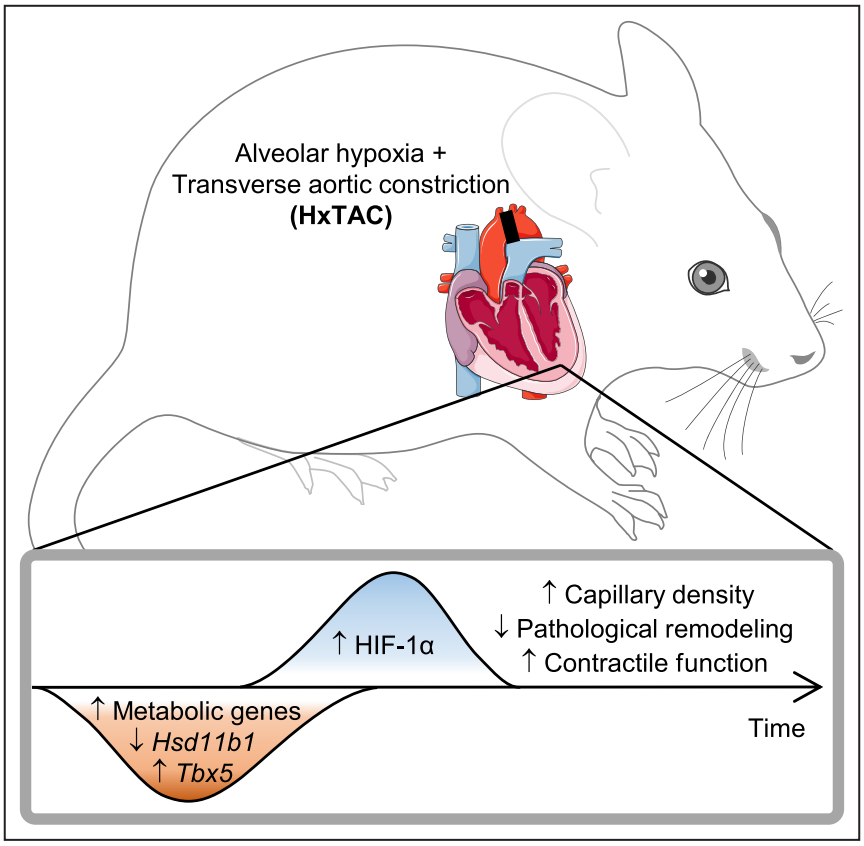

Figure 7. Summary of potential cardioprotective mechanisms in HxTAC hearts. Changes in HxTAC relative to NxTAC hearts are summarized. HIF-1α indicates hypoxia-inducible factor-1α; HxTAC, hypoxia/transverse aortic constriction; and NxTAC, normoxia/transverse aortic constriction.

with the relatively short time frame that was required to perform procedures outside the hypoxic environment. LVPO by TAC was induced after mice were adapted to alveolar hypoxia. It will be of interest to determine the impact of alveolar hypoxia on the development of HF after the induction of LVPO. These studies allow to test additional therapeutic aspects of alveolar hypoxia and might better reflect the clinical setting, in which therapeutic regimens are typically initiated after the onset of cardiac injury.

CONCLUSIONS

In summary, we present the novel HxTAC model to identify alveolar hypoxia-mediated cardioprotective mechanisms. The identified mechanisms, by which hypoxia attenuates HF under LVPO conditions comprise increased HIF-1α–mediated angiogenesis, preserved metabolic gene expression, and attenuated induction of genes that are associated with pathological remodeling. Furthermore, we identified increased *Tbx5* and decreased *Hsd11b1* expression as potential mechanisms that attenuate HF in the HxTAC model and promote LVAD-mediated myocardial recovery in HF patients (Figure 7). These data highlight the potential of the HxTAC model as a novel tool to discover hypoxia-mediated cardioprotective mechanisms and potential therapeutic targets, which might attenuate both LVPO-induced HF and mediate cardiac recovery.

ARTICLE INFORMATION

Received November 14, 2023; accepted December 27, 2023.

Affiliations

Department of Cardiology and Angiology, Hannover Medical School, Hannover, Germany (N.F., M.S., P.G., M.K.-K., D.B., M.R.R., S.G., Y.W., K.C.W., J.B., C.R.); Nora Eccles Harrison Cardiovascular Research and Training Institute (CVRTI) and Division of Cardiovascular Medicine, University of Utah School of Medicine, Salt Lake City, UT (J.R.V., R.H., S.G.D.); Institute of Pathology (C.W., M.P.K., D.D.J.) and Department of Human Genetics (W.H., M.T.), Hannover Medical School, Hannover, Germany; L3S Research Center, Leibniz University, Hannover, Germany (M.T.); Helmholtz Center for Infection Research, Research Group Genome Analytics, Braunschweig, Germany (R.G.); Division of Molecular and Cellular Pathology, Department of Pathology, University of Alabama at Birmingham, Birmingham, AL (A.R.W.); Biomedical Research in End-stage and Obstructive Lung Disease Hannover (BREATH), German Lung Research Center (DZL), Hannover, Germany (M.P.K., D.D.J.); Department of Pediatric Cardiology and Critical Care, Hannover Medical School, Hannover, Germany (G.H.); Department of Pediatric Cardiology, University Medical Center Erlangen, Friedrich-Alexander University Erlangen-Nürnberg, Erlangen,

Germany (G.H.); and Department of Medicine, David Geffen School of Medicine and UCLA Health, Los Angeles, CA (E.D.A.).

Acknowledgments

The authors thank Anna Gigina and Silke Pretzer for technical assistance and Lea Naasner for help with the analysis of mitochondrial oxygen consumption. Figure 7 was produced using templates from Servier Medical Art (https://smart.servier.com).

Sources of Funding

This work was supported by a research grant of the German Heart Foundation to C.R. (F/32/18); the German Research Foundation (DFG) and the Clinical Research Unit (KFO) 311 to D.D.J., G.H., K.C.W., and J.B.; American Heart Association Heart Failure Strategically Focused Research Network 16SFRN29020000 to S.G.D.; National Heart, Lung, and Blood Institute R01 HL135121-01 and R01 HL132067-01A1 to S.G.D.; and Nora Eccles Treadwell Foundation Grant to S.G.D.

Disclosures

None.

Supplemental Material

Data S1–S2
Tables S1–S4
Figures S1–S5
References 57–63
Data S2

REFERENCES

1. Faeh D, Gutzwiller F, Bopp M; Swiss National Cohort Study Group. Lower mortality from coronary heart disease and stroke at higher altitudes in Switzerland. *Circulation*. 2009;120:495–501. doi: 10.1161/CIRCULATIONAHA.108.819250
2. Mortimer EA Jr, Monson RR, MacMahon B. Reduction in mortality from coronary heart disease in men residing at high altitude. *N Engl J Med*. 1977;296:581–585. doi: 10.1056/NEJM197703172961101
3. Faeh D, Moser A, Panczak R, Bopp M, Roosli M, Spoerri A; Swiss National Cohort Study Group. Independent at heart: persistent association of altitude with ischaemic heart disease mortality after consideration of climate, topography and built environment. *J Epidemiol Community Health*. 2016;70:798–806. doi: 10.1136/jech-2015-206210
4. Nakada Y, Canseco DC, Thet S, Abdisalaam S, Asaithamby A, Santos CX, Shah AM, Zhang H, Faber JE, Kinter MT, et al. Hypoxia induces heart regeneration in adult mice. *Nature*. 2017;541:222–227. doi: 10.1038/nature20173
5. Honemann JN, Gerlach D, Hoffmann F, Kramer T, Weis H, Hellweg CE, Konda B, Zaha VG, Sadek HA, van Herwarden AE, et al. Hypoxia and cardiac function in patients with prior myocardial infarction. *Circ Res*. 2023;132:1165–1167. doi: 10.1161/CIRCRESAHA.122.322334
6. Semenza GL. Hydroxylation of HIF-1: oxygen sensing at the molecular level. *Physiology (Bethesda)*. 2004;19:176–182. doi: 10.1152/physiol.00001.2004
7. Kulshreshtha R, Davuluri RV, Calin GA, Ivan M. A microRNA component of the hypoxic response. *Cell Death Differ*. 2008;15:667–671. doi: 10.1038/sj.cdd.4402310
8. Peng X, Gao H, Xu R, Wang H, Mei J, Liu C. The interplay between HIF-1alpha and noncoding RNAs in cancer. *J Exp Clin Cancer Res*. 2020;39:27. doi: 10.1186/s13046-020-1535-y
9. Kido M, Du L, Sullivan CC, Li X, Deutsch R, Jamieson SW, Thistlethwaite PA. Hypoxia-inducible factor 1-alpha reduces infarction and attenuates progression of cardiac dysfunction after myocardial infarction in the mouse. *J Am Coll Cardiol*. 2005;46:2116–2124. doi: 10.1016/j.jacc.2005.08.045
10. Cai Z, Zhong H, Bosch-Marce M, Fox-Talbot K, Wang L, Wei C, Trush MA, Semenza GL. Complete loss of ischaemic preconditioning-induced cardioprotection in mice with partial deficiency of HIF-1 alpha. *Cardiovasc Res*. 2008;77:463–470. doi: 10.1093/cvr/cvm035
11. Riehle C, Bauersachs J. Small animal models of heart failure. *Cardiovasc Res*. 2019;115:1838–1849. doi: 10.1093/cvr/cvz161
12. Sano M, Minamino T, Toko H, Miyauchi H, Orimo M, Qin Y, Akazawa H, Tateno K, Kayama Y, Harada M, et al. P53-induced inhibition of HIF-1 causes cardiac dysfunction during pressure overload. *Nature*. 2007;446:444–448. doi: 10.1038/nature05602
13. Silter M, Kogler H, Zieseniss A, Wilting J, Schafer K, Toischer K, Rokita AG, Breves G, Maier LS, Katschinski DM. Impaired Ca(2+)-handling in HIF-1alpha(+/–) mice as a consequence of pressure overload. *Pflugers Arch*. 2010;459:569–577. doi: 10.1007/s00424-009-0748-x
14. Wei H, Bedja D, Koitabashi N, Xing D, Chen J, Fox-Talbot K, Rouf R, Chen S, Steenbergen C, Harmon JW, et al. Endothelial expression of hypoxia-inducible factor 1 protects the murine heart and aorta from pressure overload by suppression of TGF-beta signaling. *Proc Natl Acad Sci USA*. 2012;109:E841–E850. doi: 10.1073/pnas.1202081109
15. Krishnan J, Suter M, Windak R, Krebs T, Felley A, Montessuit C, Tokarska-Schlattner M, Aasum E, Bogdanova A, Perriard E, et al. Activation of a HIF1alpha-PPARgamma axis underlies the integration of glycolytic and lipid anabolic pathways in pathologic cardiac hypertrophy. *Cell Metabol*. 2009;9:512–524. doi: 10.1016/j.cmet.2009.05.005
16. Wever-Pinzon O, Drakos SG, McKellar SH, Horne BD, Caine WT, Kfoury AG, Li DY, Fang JC, Stehlik J, Selzman CH. Cardiac recovery during long-term left ventricular assist device support. *J Am Coll Cardiol*. 2016;68:1540–1553. doi: 10.1016/j.jacc.2016.07.743
17. Wever-Pinzon J, Selzman CH, Stoddard G, Wever-Pinzon O, Catino A, Kfoury AG, Diakos NA, Reid BB, McKellar S, Bonios M, et al. Impact of ischemic heart failure etiology on cardiac recovery during mechanical unloading. *J Am Coll Cardiol*. 2016;68:1741–1752. doi: 10.1016/j.jacc.2016.07.756
18. Drakos SG, Pagani FD, Lundberg MS, Baldwin JT. Advancing the science of myocardial recovery with mechanical circulatory support: a Working Group of the National, Heart, Lung, and Blood Institute. *JACC Basic Transl Sci*. 2017;2:335–340. doi: 10.1016/j.jacbts.2016.12.003
19. Kanwar MK, Selzman CH, Ton VK, Miera O, Cornwell WK III, Antaki J, Drakos S, Shah P. Clinical myocardial recovery in advanced heart failure with long term left ventricular assist device support. *J Heart Lung Transplant*. 2022;41:1324–1334. doi: 10.1016/j.healun.2022.05.015
20. Drakos SG, Badolia R, Makaju A, Kyriakopoulos CP, Wever-Pinzon O, Tracy CM, Bakhtina A, Bia R, Parnell T, Taleb I, et al. Distinct transcriptomic and proteomic profile specifies patients who have heart failure with potential of myocardial recovery on mechanical unloading and circulatory support. *Circulation*. 2023;147:409–424. doi: 10.1161/CIRCULATIONAHA.121.056600
21. Tseliou E, Lavine KJ, Wever-Pinzon O, Topkara VK, Meyns B, Adachi I, Zimpfer D, Birks EJ, Burkhoff D, Drakos SG. Biology of myocardial recovery in advanced heart failure with long-term mechanical support. *J Heart Lung Transplant*. 2022;41:1309–1323. doi: 10.1016/j.healun.2022.07.007
22. Grund A, Szaroszyk M, Korf-Klingebiel M, Malek Mohammadi M, Trogisch FA, Schrameck U, Gigina A, Tiedje C, Gaestel M, Kraft T, et al. TIP30 counteracts cardiac hypertrophy and failure by inhibiting translational elongation. *EMBO Mol Med*. 2019;11:e10018. doi: 10.15252/emmm.201810018
23. Legchenko E, Chouvarine P, Borchert P, Fernandez-Gonzalez A, Snay E, Meier M, Maegel L, Mitsialis SA, Rog-Zielinska EA, Kourembanas S, et al. PPARgamma agonist pioglitazone reverses pulmonary hypertension and prevents right heart failure via fatty acid oxidation. *Sci Transl Med*. 2018;10:eaao0303. doi: 10.1126/scitranslmed.aao0303
24. Li YH, Reddy AK, Ochoa LN, Pham TT, Hartley CJ, Michael LH, Entman ML, Taffet GE. Effect of age on peripheral vascular response to transverse aortic banding in mice. *J Gerontol A Biol Sci Med Sci*. 2003;58:B895–B899. doi: 10.1093/gerona/58.10.B895
25. Pacher P, Nagayama T, Mukhopadhyay P, Batkai S, Kass DA. Measurement of cardiac function using pressure-volume conductance catheter technique in mice and rats. *Nat Protoc*. 2008;3:1422–1434. doi: 10.1038/nprot.2008.138
26. Bugger H, Chen D, Riehle C, Soto J, Theobald HA, Hu XX, Ganesan B, Weimer BC, Abel ED. Tissue-specific remodeling of the mitochondrial proteome in type 1 diabetic Akita mice. *Diabetes*. 2009;58:1986–1997. doi: 10.2337/db09-0259
27. Naasner L, Froese N, Hofmann W, Galuppo P, Werlein C, Shymotiuk I, Szaroszyk M, Erschow S, Amanakis G, Bahre H, et al. Vitamin A preserves cardiac energetic gene expression in a murine model of diet-induced obesity. *Am J Physiol*. 2022;323:H1352–H1364. doi: 10.1152/ajpheart.00514.2022
28. Boudina S, Sena S, O'Neill BT, Tathireddy P, Young ME, Abel ED. Reduced mitochondrial oxidative capacity and increased mitochondrial

uncoupling impair myocardial energetics in obesity. *Circulation*. 2005;112:2686–2695. doi: 10.1161/CIRCULATIONAHA.105.554360
29. Riehle C, Weatherford ET, Wende AR, Jaishy BP, Seei AW, McCarty NS, Rech M, Shi Q, Reddy GR, Kutschke WJ, et al. Insulin receptor substrates differentially exacerbate insulin-mediated left ventricular remodeling. *JCI Insight*. 2020;5:e134920. doi: 10.1172/jci.insight.134920
30. Riehle C, Wende AR, Zaha VG, Pires KM, Wayment B, Olsen C, Bugger H, Buchanan J, Wang X, Moreira AB, et al. PGC-1beta deficiency accelerates the transition to heart failure in pressure overload hypertrophy. *Circ Res*. 2011;109:783–793. doi: 10.1161/CIRCRESAHA.111.243964
31. Semenza GL. Regulation of oxygen homeostasis by hypoxia-inducible factor 1. *Physiology (Bethesda)*. 2009;24:97–106. doi: 10.1152/physiol.00045.2008
32. Pan S, Caleshu CA, Dunn KE, Foti MJ, Moran MK, Soyinka O, Ashley EA. Cardiac structural and sarcomere genes associated with cardiomyopathy exhibit marked intolerance of genetic variation. *Circ Cardiovasc Genet*. 2012;5:602–610. doi: 10.1161/CIRCGENETICS.112.963421
33. Gupta MP. Factors controlling cardiac myosin-isoform shift during hypertrophy and heart failure. *J Mol Cell Cardiol*. 2007;43:388–403. doi: 10.1016/j.yjmcc.2007.07.045
34. Riehle C, Abel ED. PGC-1 proteins and heart failure. *Trends Cardiovasc Med*. 2012;22:98–105. doi: 10.1016/j.tcm.2012.07.003
35. Lopaschuk GD, Karwi QG, Tian R, Wende AR, Abel ED. Cardiac energy metabolism in heart failure. *Circ Res*. 2021;128:1487–1513. doi: 10.1161/CIRCRESAHA.121.318241
36. Arnolds DE, Liu F, Fahrenbach JP, Kim GH, Schillinger KJ, Smemo S, McNally EM, Nobrega MA, Patel VV, Moskowitz IP. TBX5 drives Scn5a expression to regulate cardiac conduction system function. *J Clin Invest*. 2012;122:2509–2518. doi: 10.1172/JCI62617
37. Moskowitz IP, Kim JB, Moore ML, Wolf CM, Peterson MA, Shendure J, Nobrega MA, Yokota Y, Berul C, Izumo S, et al. A molecular pathway including Id2, Tbx5, and Nkx2-5 required for cardiac conduction system development. *Cell*. 2007;129:1365–1376. doi: 10.1016/j.cell.2007.04.036
38. Garg V, Kathiriya IS, Barnes R, Schluterman MK, King IN, Butler CA, Rothrock CR, Eapen RS, Hirayama-Yamada K, Joo K, et al. GATA4 mutations cause human congenital heart defects and reveal an interaction with TBX5. *Nature*. 2003;424:443–447. doi: 10.1038/nature01827
39. McSweeney SJ, Hadoke PW, Kozak AM, Small GR, Khaled H, Walker BR, Gray GA. Improved heart function follows enhanced inflammatory cell recruitment and angiogenesis in 11betaHSD1-deficient mice post-MI. *Cardiovasc Res*. 2010;88:159–167. doi: 10.1093/cvr/cvq149
40. Small GR, Hadoke PW, Sharif I, Dover AR, Armour D, Kenyon CJ, Gray GA, Walker BR. Preventing local regeneration of glucocorticoids by 11beta-hydroxysteroid dehydrogenase type 1 enhances angiogenesis. *Proc Natl Acad Sci USA*. 2005;102:12165–12170. doi: 10.1073/pnas.0500641102
41. Kimura W, Nakada Y, Sadek HA. Hypoxia-induced myocardial regeneration. *J Appl Physiol (1985)*. 2017;123:1676–1681. doi: 10.1152/japplphysiol.00328.2017
42. Savla JJ, Levine BD, Sadek HA. The effect of hypoxia on cardiovascular disease: friend or foe? *High Alt Med Biol*. 2018;19:124–130. doi: 10.1089/ham.2018.0044
43. Ezzati M, Horwitz ME, Thomas DS, Friedman AB, Roach R, Clark T, Murray CJ, Honigman B. Altitude, life expectancy and mortality from ischaemic heart disease, stroke, copd and cancers: national population-based analysis of US counties. *J Epidemiol Community Health*. 2012;66:e17. doi: 10.1136/jech.2010.112938
44. Semenza GL. Hypoxia-inducible factor 1 and cardiovascular disease. *Ann Rev Physiol*. 2014;76:39–56. doi: 10.1146/annurev-physiol-021113-170322
45. Papandreou I, Cairns RA, Fontana L, Lim AL, Denko NC. HIF-1 mediates adaptation to hypoxia by actively downregulating mitochondrial oxygen consumption. *Cell Metabol*. 2006;3:187–197. doi: 10.1016/j.cmet.2006.01.012
46. Fukuda R, Zhang H, Kim JW, Shimoda L, Dang CV, Semenza GL. HIF-1 regulates cytochrome oxidase subunits to optimize efficiency of respiration in hypoxic cells. *Cell*. 2007;129:111–122. doi: 10.1016/j.cell.2007.01.047
47. Kim JW, Tchernyshyov I, Semenza GL, Dang CV. HIF-1-mediated expression of pyruvate dehydrogenase kinase: a metabolic switch required for cellular adaptation to hypoxia. *Cell Metabol*. 2006;3:177–185. doi: 10.1016/j.cmet.2006.02.002
48. Saeed O, Bhatia V, Formica P, Browne A, Aldrich TK, Shin JJ, Maybaum S. Improved exercise performance and skeletal muscle strength after simulated altitude exposure: a novel approach for patients with chronic heart failure. *J Card Fail*. 2012;18:387–391. doi: 10.1016/j.cardfail.2012.02.003
49. Anderson JD, Honigman B. The effect of altitude-induced hypoxia on heart disease: do acute, intermittent, and chronic exposures provide cardioprotection? *High Alt Med Biol*. 2011;12:45–55. doi: 10.1089/ham.2010.1021
50. Agostoni P. Considerations on safety and treatment of patients with chronic heart failure at high altitude. *High Alt Med Biol*. 2013;14:96–100. doi: 10.1089/ham.2012.1117
51. Marian AJ, Braunwald E. Hypertrophic cardiomyopathy: genetics, pathogenesis, clinical manifestations, diagnosis, and therapy. *Circ Res*. 2017;121:749–770. doi: 10.1161/CIRCRESAHA.117.311059
52. Steimle JD, Moskowitz IP. Tbx5: a key regulator of heart development. *Curr Top Dev Biol*. 2017;122:195–221. doi: 10.1016/bs.ctdb.2016.08.008
53. Gonzalez-Teran B, Pittman M, Felix F, Thomas R, Richmond-Buccola D, Huttenhain R, Choudhary K, Moroni E, Costa MW, Huang Y, et al. Transcription factor protein interactomes reveal genetic determinants in heart disease. *Cell*. 2022;185:794–814.e30. doi: 10.1016/j.cell.2022.01.021
54. Maitra M, Schluterman MK, Nichols HA, Richardson JA, Lo CW, Srivastava D, Garg V. Interaction of Gata4 and Gata6 with Tbx5 is critical for normal cardiac development. *Dev Biol*. 2009;326:368–377. doi: 10.1016/j.ydbio.2008.11.004
55. Gray GA, White CI, Castellan RF, McSweeney SJ, Chapman KE. Getting to the heart of intracellular glucocorticoid regeneration: 11beta-HSD1 in the myocardium. *J Mol Endocrinol*. 2017;58:R1–R13.doi: 10.1530/JME-16-0128
56. Witt H, Schubert C, Jaekel J, Fliegner D, Penkalla A, Tiemann K, Stypmann J, Roepcke S, Brokat S, Mahmoodzadeh S, et al. Sex-specific pathways in early cardiac response to pressure overload in mice. *J Mol Med (Berl)*. 2008;86:1013–1024. doi: 10.1007/s00109-008-0385-4
57. Dobin A, Davis CA, Schlesinger F, Drenkow J, Zaleski C, Jha S, Batut P, Chaisson M, Gingeras TR. STAR: ultrafast universal RNA-seq aligner. *Bioinformatics*. 2013;29:15–21. doi: 10.1093/bioinformatics/bts635
58. Liao Y, Smyth GK, Shi W. Featurecounts: an efficient general purpose program for assigning sequence reads to genomic features. *Bioinformatics*. 2014;30:923–930. doi: 10.1093/bioinformatics/btt656
59. Love MI, Huber W, Anders S. Moderated estimation of fold change and dispersion for RNA-seq data with DESeq2. *Genome Biol*. 2014;15:550. doi: 10.1186/s13059-014-0550-8
60. Ochs M, Muhlfeld C. Quantitative microscopy of the lung: a problem-based approach. Part 1: basic principles of lung stereology. *Am J Physiol Lung Cell Mol Physiol*. 2013;305:L15–L22. doi: 10.1152/ajplung.00429.2012
61. Schindelin J, Arganda-Carreras I, Frise E, Kaynig V, Longair M, Pietzsch T, Preibisch S, Rueden C, Saalfeld S, Schmid B, et al. Fiji: an open-source platform for biological-image analysis. *Nat Methods*. 2012;9:676–682. doi: 10.1038/nmeth.2019
62. Lang RM, Badano LP, Mor-Avi V, Afilalo J, Armstrong A, Ernande L, Flachskampf FA, Foster E, Goldstein SA, Kuznetsova T, et al. Recommendations for cardiac chamber quantification by echocardiography in adults: an update from the American Society of Echocardiography and the European Association of Cardiovascular Imaging. *J Am Soc Echocardiogr*. 2015;28:1–39.e14. doi: 10.1016/j.echo.2014.10.003
63. Shah P, Psotka M, Taleb I, Alharethi R, Shams MA, Wever-Pinzon O, Yin M, Latta F, Stehlik J, Fang JC, et al. Framework to classify reverse cardiac remodeling with mechanical circulatory support: the Utah-Inova stages. *Circ Heart Fail*. 2021;14:e007991. doi: 10.1161/CIRCHEARTFAILURE.120.007991